Environmental Allergens House Dust Mites-induced Asthma Causes Ferroptosis in the Lungs

Weifeng Tang
Huashan Hospital Fudan University
Ming Dong
Gumei community health center
Fangzhou Teng
Huashan Hospital Fudan University
Jie Cui
Huashan Hospital Fudan University
Xueyi Zhu
Huashan Hospital Fudan University
Wenqian Wang
Huashan Hospital Fudan University
Tulake Wuniqiemu
Huashan Hospital Fudan University
Jingjing Qin
Huashan Hospital Fudan University
La Yi
Huashan Hospital Fudan University
Shiyuan Wang
Huashan Hospital Fudan University
Jingcheng Dong
Huashan Hospital Fudan University
Ying Wei (weiying_acup@126.com)
Huashan Hospital Fudan University https://orcid.org/0000-0002-7519-6867

Research

Keywords: House dust mites, Allergic asthma, Ferroptosis, ROS, GPX4

Posted Date: February 24th, 2021

DOI: https://doi.org/10.21203/rs.3.rs-221034/v1

Abstract

Background: Studies have indicated that allergens such as house dust mites (HDM) in the environment could induce allergic asthma. Ferroptosis is a newly discovered regulatory cell death characterized by aberrant lipid peroxidation and accumulation of reactive oxygen species (ROS) in cells. However, whether ferroptosis participates in the pathological progress of asthma remains to be elucidated. In this study, we used a HDM-induced mouse asthma model to determine the effect of HDM exposure on allergic asthma and the underlying mechanisms.

Methods: Female BALB/c mice were intranasally exposed to HDM to induce allergic asthma. Airway hyperresponsiveness (AHR), lung inflammation and mucus secretion, IgE and cytokine levels as well as inflammatory cell counts in bronchalveolar lavage fluid (BALF) were investigated. In addition, the morphological changes of mitochondria, ROS, glutathione (GSH) levels and changes in ferroptosis pathway proteins in the lung were also determined.

Results: HDM exposure increased AHR significantly, and enhanced inflammatory cell infiltration and mucus secretion around the airways. Furthermore, elevated IgE level in BALF, lung eosinophilia, and a concomitant increase in IL-13 and IL-5 in BALF were observed. HDM inhalation increased ROS and decreased GSH level in the lung. HDM inhalation induced dysmorphic small mitochondria with decreased crista, as well as condensed, ruptured outer membranes. Western blot analysis demonstrated that activity of glutathione peroxidase 4 (GPX4) and catalytic subunit solute carrier family 7 member 11 (SLC7A11) decreased significantly, and protein expression of acyl-CoA synthetase long-chain family member 4 (ACSL4) and 15 Lipoxygenase 1 (15-LO1) upregulated prominently compared with mice in normal control group.

Conclusions: These in all indicated that the AHR, airway inflammation, lipid peroxidation and ROS level increased in HDM-induced asthma, and HDM inhalation caused ferroptosis in the lungs, which helped to form a better understanding of the pathogenesis of allergic asthma and targeted treatment strategies.

Background

Allergic diseases are distributed worldwide, with their risk factors and triggers varied according to geographical and environmental differences. Allergic asthma is a heterogeneous inflammatory lung disease, characterized by lung inflammation, airway hyperreactivity (AHR) and airway remodeling. According to the statistics, about 300 million people worldwide suffer from asthma[1], half of which are allergic, with the incidence continuously increasing. Inhaled corticosteroids and long acting bronchodilators are the main therapeutic drugs for asthma treatment in the clinic[2]. However, the available treatments are ineffective due to the heterogeneity of asthma and the variability in the response to the available medications[3]. Furthermore, some patients have poor symptom control and suffer from recurrent exacerbations despite strictly adhering to therapy[4]. In view of this, further mechanistic insights into the pathogenesis of asthma and better targeted treatment strategies are still needed.

Allergens such as house dust mites (HDM) in the environment are major risk factors for asthma[5]. HDM are commonly present in human dwellings and are especially abundant in mattresses, sofas, carpets and blankets. HDM can also be detected in the air, and studies using volumetric samples equipped with sizing devices have shown that mite allergens remain airborne for a short period of time. Dermatophagoides pteronyssinus (Pyroglyphidae family), usually called Der p is one of the main components in HDM, and the first identified allergen was named Der p 1, which is a glycoprotein [6]. Sensitization to HDM is a major independent risk factor for asthma in areas where the climate is conducive to mite growth[6]. It has been suggested that mite fecal pellets may occasionally enter the lung and cause inflammation and bronchoconstriction. Results have been shown that some HDM allergens may have a direct effect on bronchial epithelia, inducing inflammation through IgE-independent mechanisms[7].

Ferroptosis, which was originally observed in 2003 and formally used by Brent Stockwell, is an iron-dependent, nonapoptotic cell-death modality characterized by accumulation of lipid hydroperoxides and lipid reactive oxygen species (ROS) in cellular membranes[8, 9]. It is reported that ferroptosis is associated with mitochondrial fragmentation and cristae decrease. Ferroptotic cells do not display any hallmarks of apoptosis or necroptosis, and is determined by the balance between iron accumulation-induced ROS production and the antioxidant system that avoids lipid peroxidation. Glutathione peroxidase 4 (GPX4) is the major protective mechanism against peroxidation damage[10]. Deprivation of glutathione (GSH) could inactivate GPX4, and therefore induce ferroptosis. Organs such as kidney, brain, liver, heart and lung, are reported to be highly susceptible to ferroptosis under pathological conditions. Ferroptosis is implicated in multiple human diseases. However, whether ferroptosis participates in the pathological progression of asthma is further to be elucidated. In this study, we used a HDM-induced mouse asthma model to determine the effect of HDM exposure on allergic asthma and the underlying mechanisms associated with ferroptosis.

Materials And Methods

Animals, study protocol

Female 6–8 week old, specified-pathogen free BALB/c mice were purchased from SLAC Laboratory Animal Co., Ltd. Mice were kept under laboratory conditions (22°C, 50%-60% relative humidity, air circulation, 12h:12h light-dark cycle). Mice were randomized to two groups (10 mice/group) including normal control and HDM-induced asthma model groups. On day 0, 10μg/40μL HDM extract were administered intranasal after anesthetized with 2-2.5 % isoflurane in air. From days 7 to 11, challenge the mice daily intranasally by pipetting 40 μL of diluted HDM extract (20μg/40μL per mice) directly into the nostrils under mild anesthesia (Fig 1). For mice in normal control group, comparative volume of PBS was administered intranasally at the same time as mentioned above.

Reagents

Methacholine (Mch) and pentobarbital sodium were purchased from Sigma-Aldrich. Isoflurane was purchased from Shenzhen Ruiwode Life Technology Co. Ltd. HDM extract (Dermatophagoides pteronyssinus) was purchased from Greer Laboratories. Mouse lung dissociation kit was purchased from Milteny Biotec. Live APC-Cy7 solution and anti-mouse CD45 eF506 antibody were purchased from Thermo Fisher Scientific. Anti-mouse CD11b BV711 and anti-mouse SiglecF BV421 antibodies were purchased from BD Pharmingen. Anti-mouse Ly6C PE antibody was purchased from BioLegend. Anti-GPX4 and anti-15 Lipoxygenase 1 (15-LO1) antibodies were purchased from abcam, and anti-acyl-CoA synthetase long-chain family member 4 (ACSL4) and anti-catalytic subunit solute carrier family 7 member 11 (SLC7A11) antibodies were purchased from Novus. Monoclonal GPX4 antibody for immunohistochemistry assay was purchased from Novus. The GSH assay kit was purchased from Nanjing Jiancheng Bioengineering Institute and the reactive oxygen species (ROS) assay kit was purchased from Sigma-Aldrich. IgE, IL-5 and IL-13 Enzyme-linked immunosorbent assay (ELISA) kits were purchased from Multisciences (LIANKE) biotech. RIPA lysis buffer was purchased from Beyotime Biotechnology. BCA protein test kit was purchased from Thermo Fisher Scientific. Immobilon Western Chemiluminescent HRP Substrate was purchased from Merck.

Measurement of AHR

Within 24h after the final HDM challenge, airway hyperresponsiveness (AHR) presented as airway resistance (R_L) and dynamic lung compliance (Cdyn) to Mch were measured according to the manufacturer's instructions. Briefly, mouse was weighed, intraperitoneally anesthetized with pentobarbital sodium (50 mg/kg), incised and tracheal intubated. Afterwards, mouse was placed in the chamber, and the tracheal intubation was connected to the ventilator. AHR was challenged with increasing doses of Mch (0, 6.25, 12.5, 50, 100mg/ml), and data was recorded and presented as changes in R_L and Cdyn.

Histological analysis

Hematoxylin and eosin (HE) and periodic acid Schiff (PAS) staining were performed to determine the inflammatory and mucus secretion changes. Briefly, the middle lobe of left lung from each mouse was removed, fixed in 4% paraformaldehyde, decalcified in EDTA, dehydrated in a graded series of ethanol solutions, and embedded in paraffin. Afterwards, lung tissue sections were sectioned to slices with thickness of 4μm. Lung slices were stained with H&E and PAS solution. A semi-quantitative grading method was used to evaluate the degree of peribronchial inflammation. PAS-positive cells in the airway were counted and their percentage was calculated in the airway epithelial cells. The data was collected by three independent blinded investigators.

Electron microscopy

Changes in mitochondrial structure were observed by transmission electron microscope (TEM). Mouse lung was cut into 1×1×3 mm3 and fixed in 2.5% glutaraldehyde phosphate buffer. Fixed samples were dehydrated with ethanol and acetone, embedded and dried. Afterward, the tissue was cut into 70 nm-thick sections, stained with uranyl acetate and citrate, and visualized with the JEM-1400 Plus transmission electron microscope (Japan Electron Optics Laboratory).

Leukocyte differential counts in BALF

Bronchalveolar lavage fluid (BALF) was collected by flushing the right lungs three times with 1 mL of PBS via a 1 mL syringe inserted in the cannula. BALF was centrifuged for 10 min at 500 × g and 4 °C, and the supernatant was collected for cytokines assay and the pellet containing the cells were resuspend in 100 μL PBS for leukocyte differential counts using BC-5000 Vet (MINDRAY, China).

Cytokines in BALF

IgE and T helper (Th) 2 cells played a pathogenic role in asthma. The levels of IgE, Th2 cytokines IL-5 and IL-13 in supernatants of BALF were investigated by using sandwich ELISA kits according to the manufacturer’s instructions.

Flow cytomerty of lung tissue

Eosinophil (Eos) has been implicated in the pathogenesis of asthma. Eos population in the lung tissue was detected by flow cytomerty. CD45+CD11b+Ly6C-SiglecF+ cells were identified as EOS population in our experiment. Mouse lung dissociation kit was used to dissociate the upper right lobe of each lung to single cells. Afterwards, the single cells were stained with the fluorescently labeled solutions and antibodies (Live APC-Cy7, CD45 eF506, CD11b BV711, SiglecF BV421, Ly6C PE) and detected by an Attune NxT instrument (Thermo Fisher Scientific).

ROS and GSH measurement

Ferroptosis is determined by the balance between iron accumulation-induced ROS production and the antioxidant system that avoids lipid peroxidation[11]. In our study, the ROS and GSH levels were determined using commercial ROS and GSH assay kit according to the manufacturer's instructions.

Western blot assay

GPX4, ACSL4, 15-LO1 and SLC7A11 were mediators of lipid peroxidation and ferroptosis, and were reported to be involved in ferroptosis pathway. The expression levels of these proteins were assayed by

western blot. Lung tissues were homogenated and sonicated in RIPA lysis buffer, and centrifuged at 12000 rpm for 10 min at 4C. Afterwards, the supernatants were collected to measure the total protein level using BCA protein test kit. A 12% sodium dodecyl sulfate-polyacrylamide gelelectrophoresis (SDS-PAGE) separation gel was prepared for protein separation and transferred to PVDF membranes, followed by blockage in 5% non-fat milk at room temperature. Afterwards, the membranes were washed with Tris buffered saline tween (TBST) every 10 min for three times. After that, the PVDF membranes were incubated with GPX4(1:1000 dilution), ACSL4 (1:1000 dilution), 15-LO1 (1:1000 dilution) and SLC7A11 (1:1000 dilution) antibodies at 4℃ overnight. After three times of washing with TBST, the PVDF membranes were incubated with secondary antibodies for 1.5h at room temperature. Immobilon western chemiluminescent HRP substrate solution was used to exhibit protein band after three times of washing with TBST. β-actin was used as the internal control for the normalization of the data.

Statistical analysis

All data were analyzed and graphed by GraphPad Prism 8 (GraphPad Software, La Jolla, CA, USA). Data were presented as the mean ± standard deviation (mean ± SD). Student's t-test was used to analyze the difference between two samples. A P-value less than 0.05 was considered statistically significant.

Results

HDM exposure induced an increase in AHR to Mch

The changes in AHR were investigated. Compared with mice in normal control group, the airway resistance (R_L) increased significantly ($p<0.05$ or $p<0001$, Fig 2A, C-F) and dynamic lung compliance (Cdyn) decreased markedly ($p<0.05$ or $p<001$, Fig 2B, G-J) with Mch dose increase. There was no obvious increase in R_L between the two groups when doses of Mch less than 50 mg/ml (Fig 2C-D). With Mch dose increase (50 mg/ml and 100 mg/ml, Fig 2E-F), Mch challenge resulted in prominent augmentation of R_L. At Mch doses of 12.5, 50 and 100 mg/ml (Fig 2H-J), HDM inhalation could induce decrease in Cdyn. These data indicated that HDM exposure could aggravate AHR.

HDM exposure promoted lung inflammation and goblet cell hyperplasia

H&E staining was performed to evaluate the inflammatory changes in the lung. Our results revealed that inflammatory cell infiltration around the bronchus (Fig 3A-B) was observed in mice receiving HDM inhalation, and HDM exposure aggravated pulmonary inflammatory response. Mucus hypersecretion is an important feature of allergic asthma. Furthermore, PAS staining was conducted to evaluate the degree of goblet cell metaplasia and mucus secretion. As is shown in Fig 3A and 3C, the mucus secretion increased significantly compared with mice in the normal control group. In addition, inflammatory cells in

BALF were also detected, and our results demonstrated that the total leukocytes, lymphocytes (Lym), Eos and monocytes (Mon) increased significantly after HDM exposure ($p<0.05$, Fig 3D).

HDM inhalation enhanced airway eosinophilic and Th2 biased inflammation

CD45+CD11b+Ly6C-SiglecF+Eos population in the lung tissue was detected by flow cytomerty. Mice in HDM-induced asthma group demonstrated markedly increased CD45+CD11b+Ly6C-SiglecF+Eos propotion ($p<0.01$, Fig 4A-B). Furthermore, IgE, IL-5 and IL-13 levels in BALF were also investigated by ELISA assay. Elevated IgE, IL-5 and IL-13 levels were detected compared with mice in normal control group ($p<0.05$ or $p<0.01$ or $p<0.001$, Fig 4C-E).

HDM exposure induced ferroptosis in the lung

It is reported that ferroptosis is associated with mitochondrial fragmentation and cristae decrease[12]. To explore the role of HDM inhalation in ferroptosis, morphological changes of mitochondria were observed by TEM. Consistent with literature reports, dysmorphic small mitochondria were observed in the lung cells after HDM inhalation. Representative results were shown in Fig. 5D. Decreased mitochondria crista, condensed and ruptured outer membranes were also discovered in the lung cells of mice in HDM-induced asthma group. Imbalance between ROS production and the antioxidant system contributed to ferroptosis. Our data revealed that HDM exposure resulted in elevated ROS (Fig. 5A-B, $p<0.05$) level and reduced GSH (Fig. 5C, $p<0.05$) level in the lung tissue compared with mice exposure to PBS. These results proved that HDM exposure could induce ferroptosis in the lung.

HDM exposure induced dysregulation of proteins associated with ferroptosis pathway

To investigate the underlying mechanisms associated with ferroptosis, we measured key proteins involved in ferroptosis. The protein expression level of GPX4, ACSL4, 15-LO1 and SLC7A11 were detected. The results showed that mice receiving HDM inhalation had downregulated activity of GPX4 both from western blot and immunohistochemistry assay results (Fig 6). Furthermore, a significant upregulation of ACSL4 and 15-LO1 as well as downregulation of SLC7A11 were detected in HDM-induced asthma mice. These results demonstrated that GPX4, ACSL4, 15-LO1 and SLC7A11 were involved in ferroptosis in the lung of HDM-induced asthma mice.

Discussion

Asthma is a heterogeneous chronic inflammatory disease of the airways characterized by chronic airway inflammation, bronchoconstriction, AHR, and mucus hypersecretion[13, 14]. Recent studies revealed that

asthma was a very heterogeneous disease with multiple phenotypes and endotypes. Allergic asthma accounts for the most common form of asthma, and can be triggered by allergens in the environment, such as HDM. As naturally occurring allergens in the environment, HDM is frequently used for the preparation of allergic mouse asthma model to uncover the key inflammatory pathways in the progress of allergic asthma. In our study, we used a HDM-induced mouse asthma model to determine the effect of HDM exposure on allergic asthma and the underlying mechanisms. Our results demonstrated that intranasally administered with HDM induced AHR compared with mice exposed to PBS. Asthma is characterized by chronic inflammation in the airways. In order to observe the inflammatory changes in the airways, we performed HE and PAS staining of the lung slices. Inflammatory cell infiltration around the bronchus in the lung tissue, goblet cell metaplasia and mucus hypersecretion were obserbed after HDM inhalation. Furthermore, total leukocytes, Lym, Eos and Mon increased significantly after HDM exposure, indicating the lung inflammation induced by HDM. In addition, we detected

CD45 + CD11b + Ly6C-SiglecF + Eos population in the lung tissue, consistent with BALF leukocytes classification results, mice in HDM-induced asthma group demonstrated markedly increased CD45 + CD11b + Ly6C-SiglecF + Eos propotion. IgE and T helper (Th) 2 cells played a pathogenic role in asthma. We further investigated the levels of IgE, Th2 cytokines IL-5 and IL-13 in supernatants of BALF. It has been shown that the cysteine protease activity of Der p 1 in HDM seems to selectively enhance the IgE response and upregulate the IgE synthesis by cleaving the low-affinity IgE receptor (CD23) from the surface of human B cell lymphocytes[15]. It is reported that allergic asthma accounts for about 80 % of asthma cases, and high levels of Th2 cytokines could be detected in lung tissue and BALF. Mounting evidence has demonstrated that IL-5 and IL-13 play a prominent role in eosinophil activation and mucus hyperplasia[16, 17]. Consistent with former report, our results revealed that mice exposure to HDM had elevated IgE, IL-5 and IL-13 levels compared with mice receiving PBS. These in all indicated that HDM inhalation induced AHR and type 2 airway inflammation in asthma.

Ferroptosis is an iron-dependent cell-death modality driven by oxidative phospholipid damage and has been implicated in a number of diseases[18, 19]. In our study, we investigated whether ferroptosis participated in the pathological progression of HDM induced asthma. Mitochondria are reported to be involved in cysteine-deprivation-induced ferroptosis[20]. Morphological changes of mitochondria which include mitochondrial fragmentation and cristae decrease were observed in ferroptosis[12], and some potent ferroptosis inhibitors were demonstrated to be exquisitely targeted to mitochondria[21]. Previous study showed that lipid ROS was crucial for ferroptosis[9], indicating that accumulation of ROS is a key feature of ferroptosis. Mitochondria are major organelle for cellular ROS production. A decreased level of lipid ROS accumulation were observed in mitochondria-depleted cell[20], which further confirmed involvement of mitochondria in ferroptosis. In our study, morphological changes of mitochondria were observed by TEM, and our results revealed that decreased mitochondria crista, condensed and ruptured outer membranes were observed in the lung cells of mice in HDM-induced asthma group, which was consistent with previous results.

Polyunsaturated fatty acids (PUFAs) are the primary targets of lipid peroxidation of cell membranes. The activity of multiple upstream cascades dertermine the sensitivity to ferroptosis, which include free PUFAs as well as balance between levels of pro-oxidant factors (ROS, lipoxogynases) and antioxidant factors (GPX4, GSH). GSH is an anti-oxidant that serves as a cofactor for reduction of lipid hydroperoxides by GPX4[22]. It is reported that depletion of GSH by erastin inactivates GPX4, leading to accumulation of lipid ROS and lipid peroxidation[23]. Inhibition of GSH synthesis induces ferroptosis in some cells. In our study, ROS and GSH levels in the lung were detected, and results demonstrated that HMD exposure induced increased ROS production and reduced the levels of GSH in the lung tissue, indicating that HDM exposure might result in the imbalance between pro-oxidant and pro-oxidant factors in the lung. GPX4 is an enzyme required for the clearance of lipid ROS. GPX4 catalyses GSH to eliminate the production of phospholipid hydroperoxides (PLOOH), and the latter is the major mediator of chain reactions in lipoxygenases[11]. As the most downstream component of the ferroptosis pathway, inactivation of GPX4 was reported to result in ferroptosis even when cellular cysteine and GSH contents were normal[24]. The GPX4 activity was assessed by western blot assay in our experiment. The results showed that mice receiving HDM inhalation had downregulated activity of GPX4. ACSL4 functions to preferentially activate long PUFAs for phospholipid biosynthesis. The synthesis of long chain PUFA-CoA was inhibited in $ACSL4^{-/-}$ cells, supporting a function of ACSL4 for lipid biosynthesis. The upregulation of ACSL4, but not other ACSL members, is an essential component for ferroptosis [12, 25]. Resistance to ferroptosis was observed in GPX4/ACSL4 double knockout cells. Previous results showed that ACSL4 inhibition could be used as a therapeutic approach to prevent ferroptosis-related diseases. We also investigated effect of HDM inhalation on ACSL4 expression, and upregulation of ACSL4 was observed in HDM-induced asthma, indicating the augmentation of lipid biosynthesis by HDM inhalation. Lipoxygenases (Los) are effective in oxygenation of free PUFA. 15LO1 is highly expressed in human airway epithelial cells[26]. Recent study revealed that 15LO1 expression increased in Th2 inflammation in asthma[27]. Airway epithelial cells isolated from stable, non-exacerbating asthmatic patients had elevated 15LO1 level, which was correlated with fraction of exhaled NO, one of the key markers of Th2 inflammation [28]. We detected the 15LO1 level in the lung tissue of mice exposure to HDM, and an increase of 15LO1 protein expression level was found, which were identical with those reported in literature. As a component of the cystine/glutamate antiporter system Xc^-, SLC7A11 is essential for the exchange of extracellular cystine and intracellular glutamate across the plasma membrane, therefore providing adequate cystine within cells. Cystine in the cells is further reduced to cysteine, which is an essential precursor required for GSH synthesis. Ferroptosis can be initiated by depletion of cellular cysteine through inhibition of cystine uptake mediated by SLC7A11[29, 30]. Previous results showed that SLC7A11 downregulation significantly increased the susceptibility to ferroptosis in nascent neoplastic cells, thus keeping tumorigenesis in check. Downregulation of SLC7A11 was detected in HDM-induced asthma, consistent with its role in ferroptosis. These data proved that ferroptosis was induced in HDM induced mouse asthma model, and ROS, GSH, GPX4, ACSL4, 15LO1 and SLC7A11 were involved in ferroptosis in the lung of HDM-induced asthma mice (Fig. 7).

Conclusion

In summary, our study demonstrated that AHR, airway inflammation, lipid peroxidation and ROS level increased in HDM-induced asthma, and HDM inhalation caused ferroptosis in the lungs, which helped to form a better understanding of the pathogenesis of allergic asthma and targeted treatment strategies.

Declarations

Acknowledgments

None declared.

Ethics approval and consent to participate

The experimental procedures were approved by the Ethics Committee of Animal Experiments of Fudan University (authorization number: 2020-10-HSYY-WY-01).

Authors' contributions

Jingcheng Dong and Ying Wei: Conceptualization, Methodology, Software. Weifeng Tang and Ming Dong: Data curation, Writing-Original draft preparation. Weifeng Tang, Ming Dong, Fangzhou Teng, Jie Cui, Xueyi Zhu, Wenqian Wang, Tulake Wuniqiemu, Jingjing Qin, La Yi, and Shiyuan Wang: Visualization, Investigation. Jingcheng Dong and Ying Wei: Writing- Reviewing and Editing.

Funding

This work was supported by grants from Young Elite Scientists Sponsorship Program by China Association for Science and Technology (grant no. 2018QNRC001), the National Natural Science Foundation of China (Grant No. 81704154).

Availability of data and materials

The datasets used and/or analyzed during the current study are available from the corresponding author on reasonable request.

Consent for publication

Not applicable.

Declaration of competing interests

The authors declare that they have no known competing financial interests or personal relationships that could have appeared to influence the work reported in this paper.

References

1. Rogliani P, Calzetta L, Matera MG, Laitano R, Ritondo BL, Hanania NA, Cazzola M: **Severe Asthma and Biological Therapy: When, Which, and for Whom**. *Pulm Ther* 2020, **6**(1):47-66.
2. Calzetta L, Matera MG, Coppola A, Rogliani P: **Prospects for severe asthma treatment**. *Curr Opin Pharmacol* 2020, **56**:52-60.
3. Reddel HK, Bateman ED, Becker A, Boulet LP, Cruz AA, Drazen JM, Haahtela T, Hurd SS, Inoue H, de Jongste JC *et al*: **A summary of the new GINA strategy: a roadmap to asthma control**. *Eur Respir J* 2015, **46**(3):622-639.
4. Sulaiman I, Greene G, MacHale E, Seheult J, Mokoka M, D'Arcy S, Taylor T, Murphy DM, Hunt E, Lane SJ *et al*: **A randomised clinical trial of feedback on inhaler adherence and technique in patients with severe uncontrolled asthma**. *Eur Respir J* 2018, **51**(1).
5. Caraballo L: **Mite allergens**. *Expert Rev Clin Immunol* 2017, **13**(4):297-299.
6. Fernandez-Caldas E, Puerta L, Caraballo L: **Mites and allergy**. *Chem Immunol Allergy* 2014, **100**:234-242.
7. Jacquet A: **Interactions of airway epithelium with protease allergens in the allergic response**. *Clinical and experimental allergy : journal of the British Society for Allergy and Clinical Immunology* 2011, **41**(3):305-311.
8. Dolma S, Lessnick SL, Hahn WC, Stockwell BR: **Identification of genotype-selective antitumor agents using synthetic lethal chemical screening in engineered human tumor cells**. *Cancer Cell* 2003, **3**(3):285-296.
9. Dixon SJ, Lemberg KM, Lamprecht MR, Skouta R, Zaitsev EM, Gleason CE, Patel DN, Bauer AJ, Cantley AM, Yang WS *et al*: **Ferroptosis: an iron-dependent form of nonapoptotic cell death**. *Cell* 2012, **149**(5):1060-1072.
10. Friedmann Angeli JP, Schneider M, Proneth B, Tyurina YY, Tyurin VA, Hammond VJ, Herbach N, Aichler M, Walch A, Eggenhofer E *et al*: **Inactivation of the ferroptosis regulator Gpx4 triggers acute renal failure in mice**. *Nat Cell Biol* 2014, **16**(12):1180-1191.
11. Tang D, Kang R, Berghe TV, Vandenabeele P, Kroemer G: **The molecular machinery of regulated cell death**. *Cell Res* 2019, **29**(5):347-364.
12. Doll S, Proneth B, Tyurina YY, Panzilius E, Kobayashi S, Ingold I, Irmler M, Beckers J, Aichler M, Walch A *et al*: **ACSL4 dictates ferroptosis sensitivity by shaping cellular lipid composition**. *Nat Chem Biol* 2017, **13**(1):91-98.
13. Ish P, Malhotra N, Gupta N: **GINA 2020: what's new and why?** *J Asthma* 2020:1-5.
14. Hogan AD, Bernstein JA: **GINA updated 2019: Landmark changes recommended for asthma management**. *Ann Allergy Asthma Immunol* 2020, **124**(4):311-313.

15. Gough L, Sewell HF, Shakib F: **The proteolytic activity of the major dust mite allergen Der p 1 enhances the IgE antibody response to a bystander antigen**. *Clinical and experimental allergy : journal of the British Society for Allergy and Clinical Immunology* 2001, **31**(10):1594-1598.
16. Lambrecht BN, Hammad H, Fahy JV: **The Cytokines of Asthma**. *Immunity* 2019, **50**(4):975-991.
17. Bush A: **Cytokines and Chemokines as Biomarkers of Future Asthma**. *Front Pediatr* 2019, **7**:72.
18. Zou Y, Schreiber SL: **Progress in Understanding Ferroptosis and Challenges in Its Targeting for Therapeutic Benefit**. *Cell Chem Biol* 2020, **27**(4):463-471.
19. Gao M, Jiang X: **To eat or not to eat-the metabolic flavor of ferroptosis**. *Curr Opin Cell Biol* 2018, **51**:58-64.
20. Gao M, Yi J, Zhu J, Minikes AM, Monian P, Thompson CB, Jiang X: **Role of Mitochondria in Ferroptosis**. *Mol Cell* 2019, **73**(2):354-363 e353.
21. Krainz T, Gaschler MM, Lim C, Sacher JR, Stockwell BR, Wipf P: **A Mitochondrial-Targeted Nitroxide Is a Potent Inhibitor of Ferroptosis**. *ACS Cent Sci* 2016, **2**(9):653-659.
22. Lu SC: **Regulation of glutathione synthesis**. *Mol Aspects Med* 2009, **30**(1-2):42-59.
23. Dixon SJ, Stockwell BR: **The role of iron and reactive oxygen species in cell death**. *Nat Chem Biol* 2014, **10**(1):9-17.
24. Ingold I, Berndt C, Schmitt S, Doll S, Poschmann G, Buday K, Roveri A, Peng X, Porto Freitas F, Seibt T *et al*: **Selenium Utilization by GPX4 Is Required to Prevent Hydroperoxide-Induced Ferroptosis**. *Cell* 2018, **172**(3):409-422 e421.
25. Xu Y, Li X, Cheng Y, Yang M, Wang R: **Inhibition of ACSL4 attenuates ferroptotic damage after pulmonary ischemia-reperfusion**. *FASEB J* 2020, **34**(12):16262-16275.
26. Wenzel SE, Tyurina YY, Zhao J, St Croix CM, Dar HH, Mao G, Tyurin VA, Anthonymuthu TS, Kapralov AA, Amoscato AA *et al*: **PEBP1 Wardens Ferroptosis by Enabling Lipoxygenase Generation of Lipid Death Signals**. *Cell* 2017, **171**(3):628-641 e626.
27. Zhao J, O'Donnell VB, Balzar S, St Croix CM, Trudeau JB, Wenzel SE: **15-Lipoxygenase 1 interacts with phosphatidylethanolamine-binding protein to regulate MAPK signaling in human airway epithelial cells**. *Proc Natl Acad Sci U S A* 2011, **108**(34):14246-14251.
28. Wenzel SE: **Asthma phenotypes: the evolution from clinical to molecular approaches**. *Nat Med* 2012, **18**(5):716-725.
29. Xu X, Zhang X, Wei C, Zheng D, Lu X, Yang Y, Luo A, Zhang K, Duan X, Wang Y: **Targeting SLC7A11 specifically suppresses the progression of colorectal cancer stem cells via inducing ferroptosis**. *Eur J Pharm Sci* 2020, **152**:105450.
30. Zhang Y, Zhuang L, Gan B: **BAP1 suppresses tumor development by inducing ferroptosis upon SLC7A11 repression**. *Mol Cell Oncol* 2019, **6**(1):1536845.

Figures

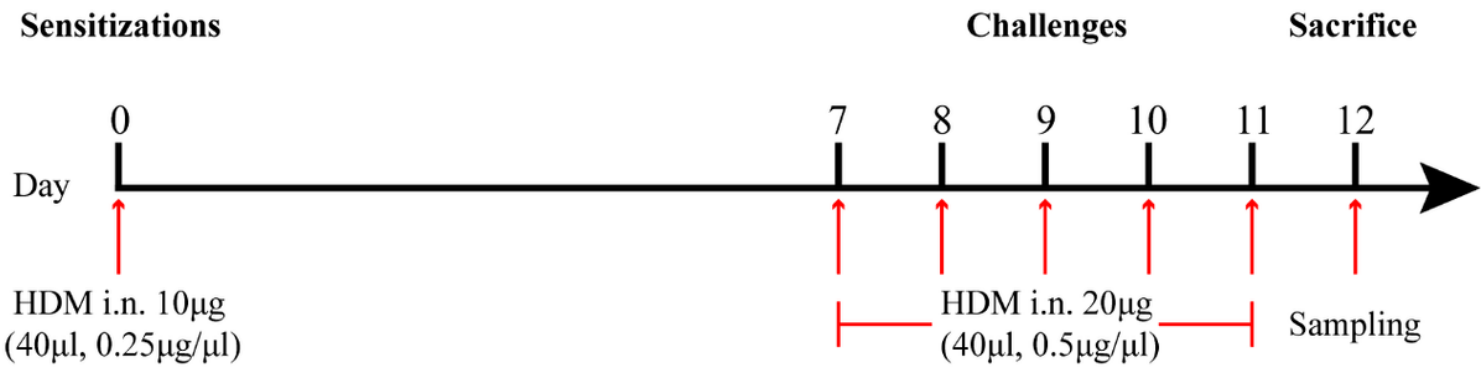

Figure 1

Protocol of preparation of HDM induced asthma model

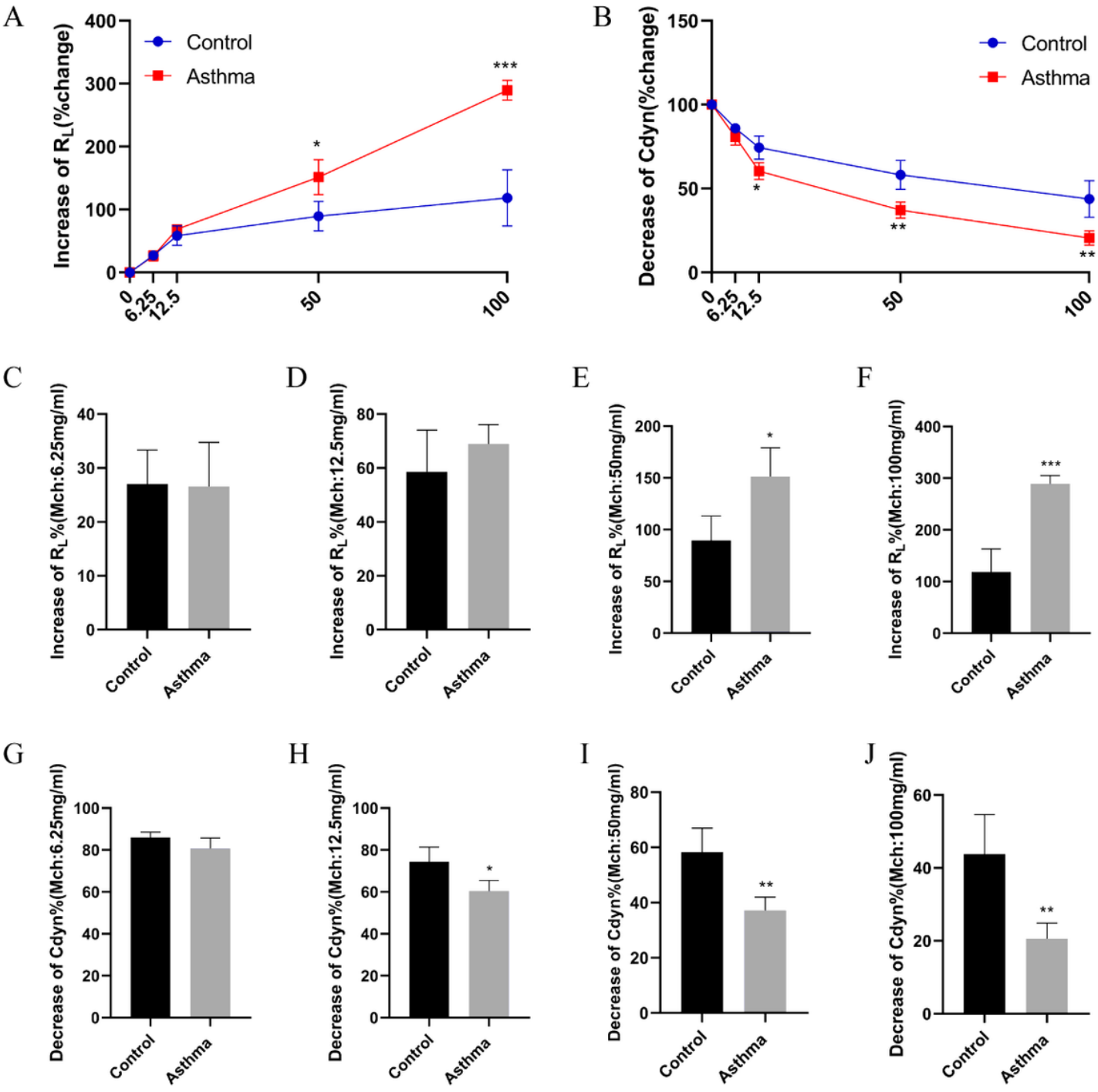

Figure 2

HDM exposure induced increase in AHR. A. Changes in airway resistance (RL). B. Changes in dynamic lung compliance (Cdyn). C-F. Changes in RL at different Mch dose. G-J. Changes in Cdyn at different Mch dose. *P < 0.05, **P < 0.01, ***P < 0.001.

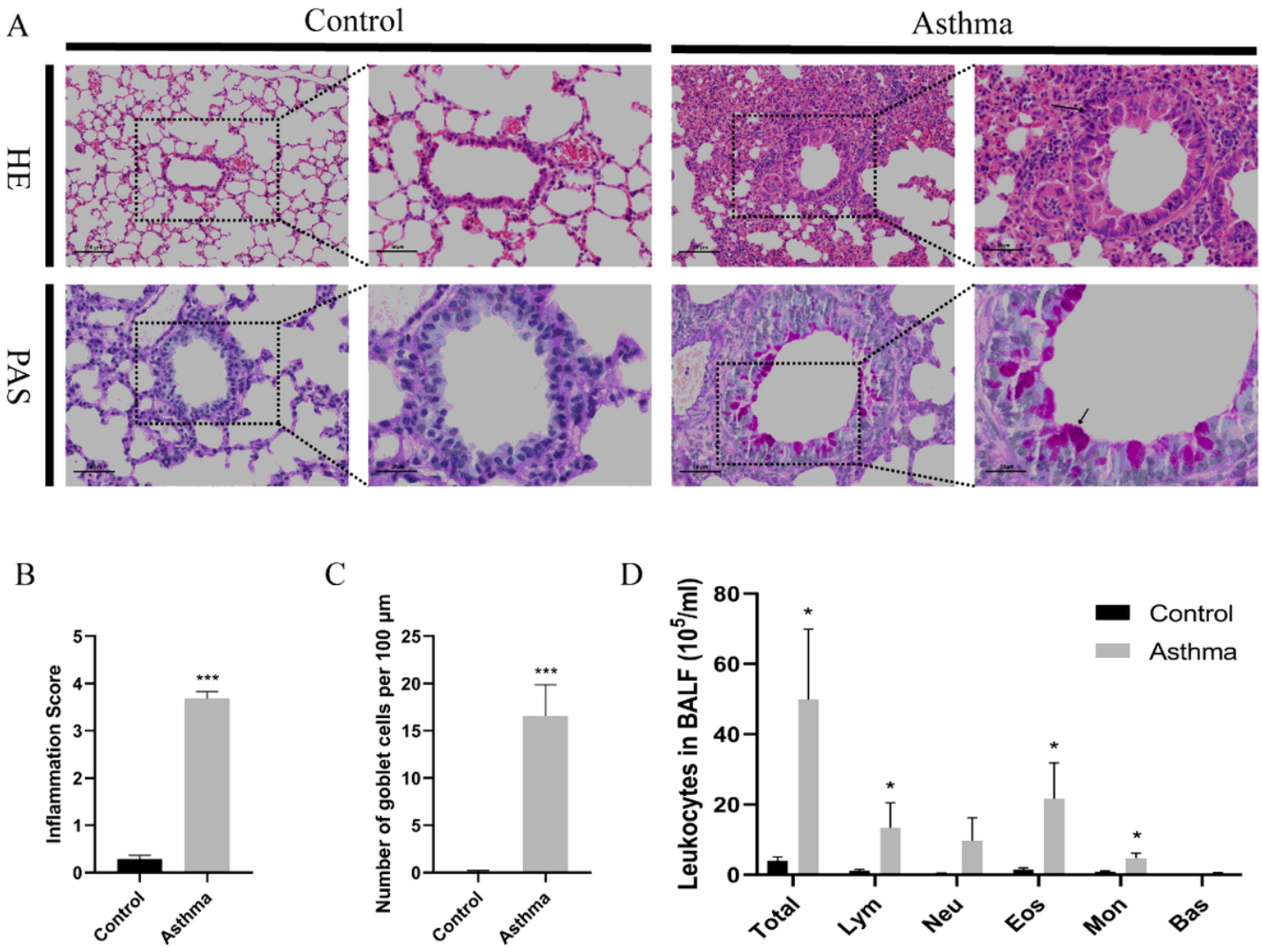

Figure 3

HDM exposure induced promoted lung inflammation and goblet cell hyperplasia. A. Representative images of HE and PAS staining results. B. Inflammation score of the HE results. C. Changes in goblet cell counts. D. Leukocytes classification in BALF. Lymphocytes (Lym), Eosinophils (Eos) and monocytes (Mon). *P < 0.05, ***P < 0.001.

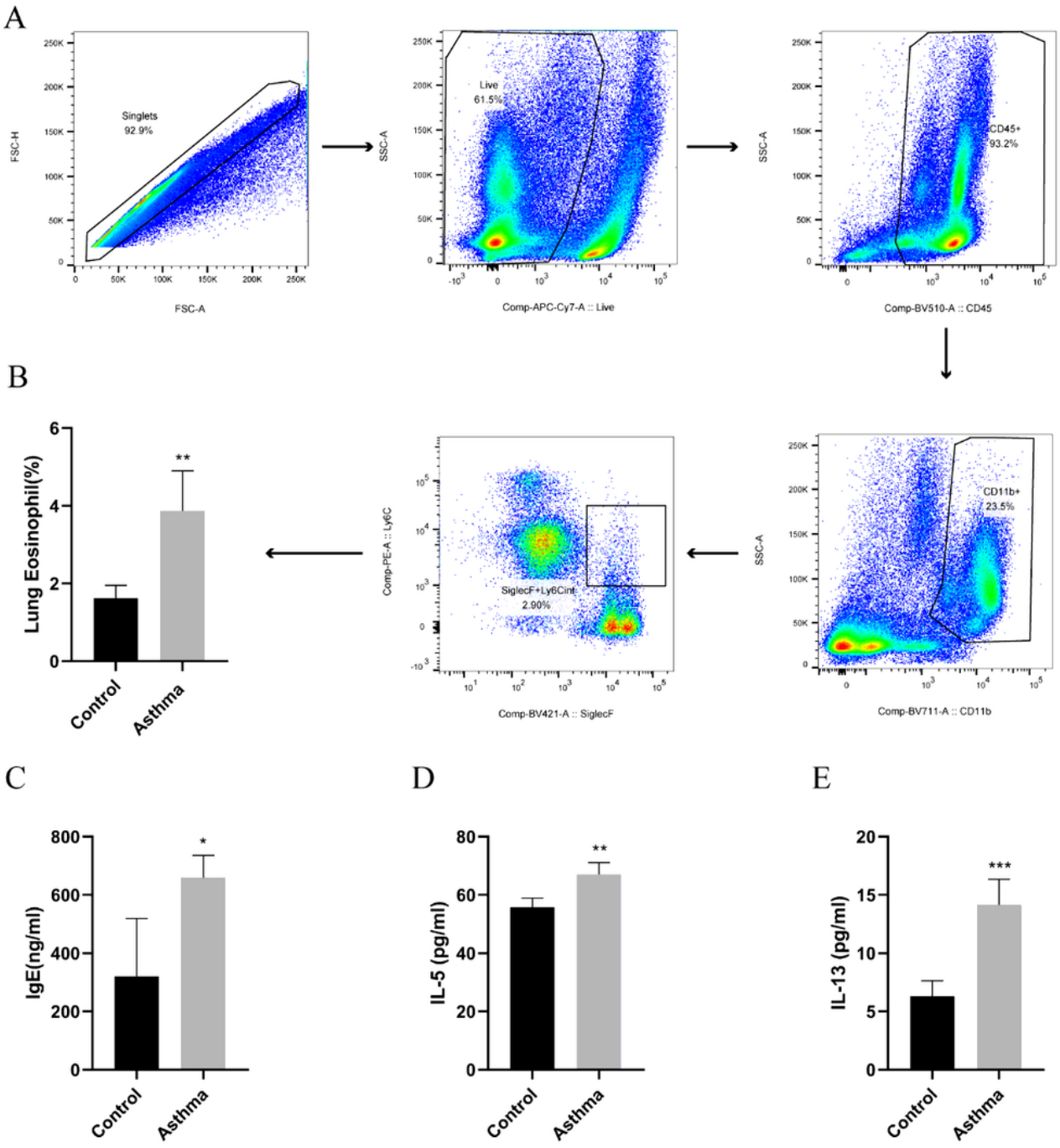

Figure 4

HDM exposure induced airway eosinophilic and Th2 biased inflammation. A. Procedure of flow cytomerty analysis of Eos in the lung. B. Changes in CD45+CD11b+Ly6C-SiglecF+Eos propotion presented by bar graph. C-E. The IgE, IL-5 and IL-13 levels in BALF. *P < 0.05, **P < 0.01, ***P < 0.001.

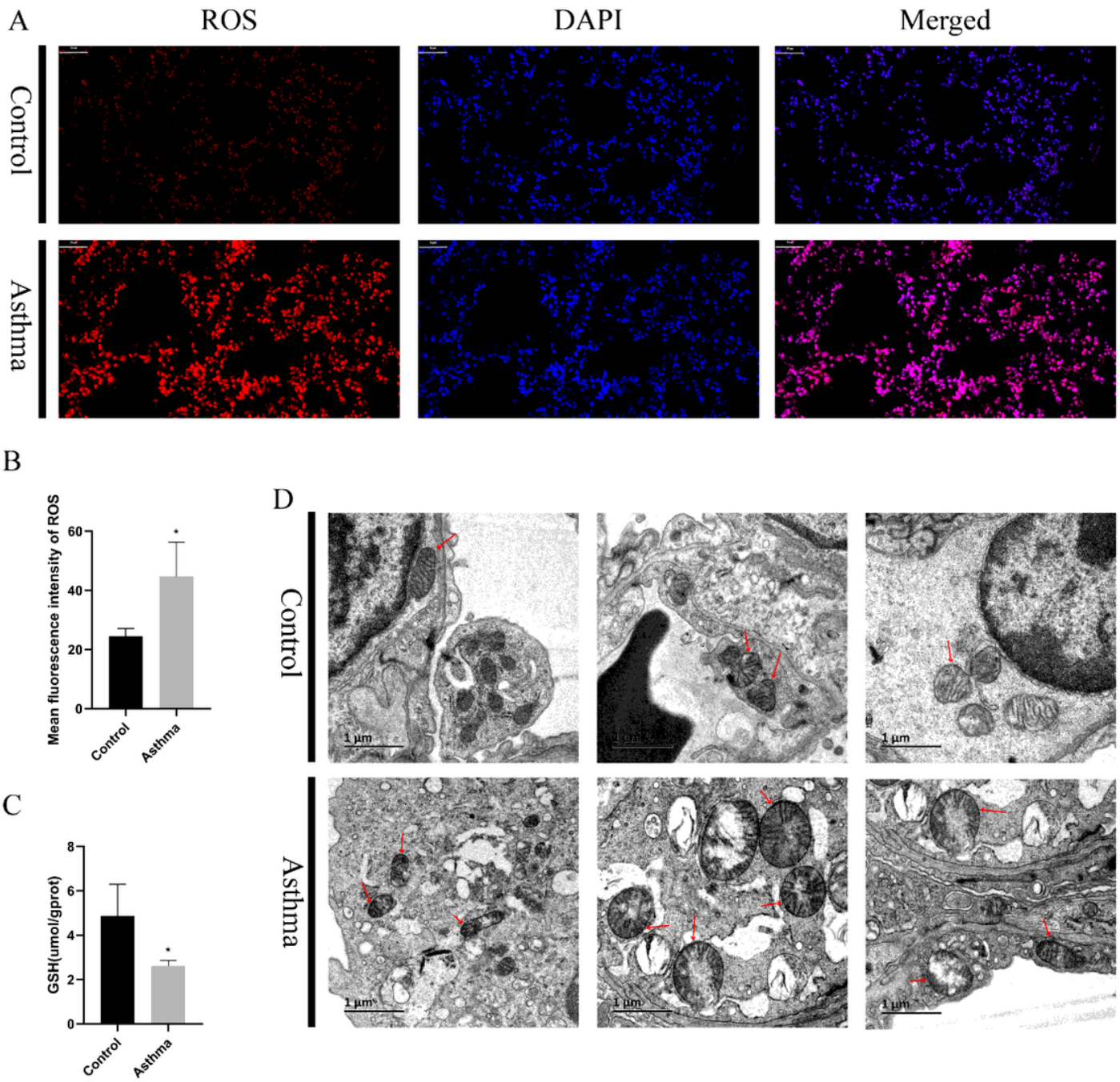

Figure 5

HDM exposure induced ferroptosis in the lung. A-B. ROS production in the lung. C. GSH level in the lung. D. Morphological changes of mitochondria in ferroptosis after HDM exposure. *P < 0.05.

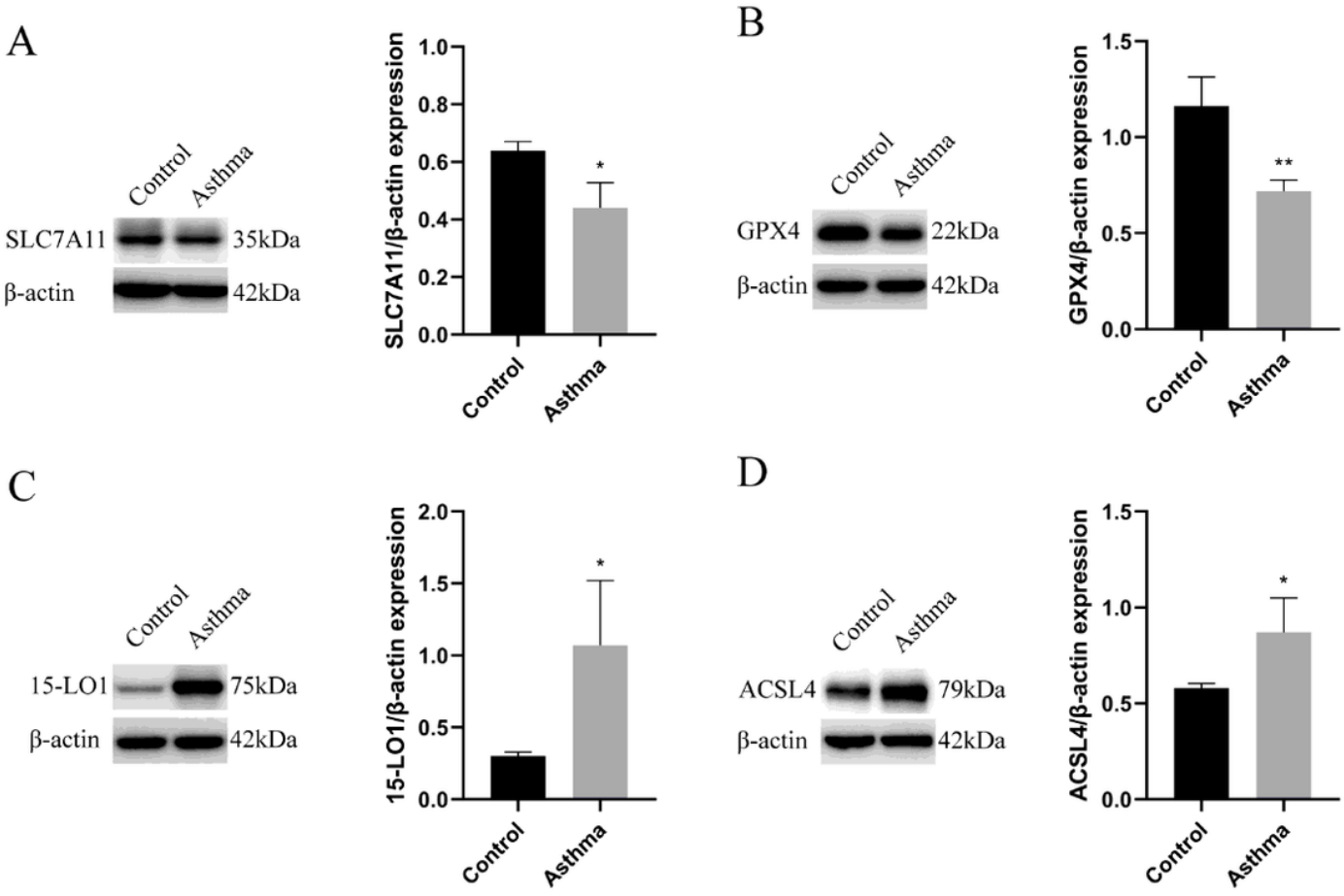

Figure 6

HDM exposure induced dysregulation of proteins associated with ferroptosis pathway. Actin was used as the loading Control. Quantitative analysis was performed from three independent experiments with Image J. A. Representative image and bar graph of western blot assay for SLC7A11. B. Representative image and bar graph of western blot assay for GPX4. C. Representative image and bar graph of western blot assay for 15-LO1. D. Representative image and bar graph of western blot assay for ASCL4. *P < 0.05, **P < 0.01.

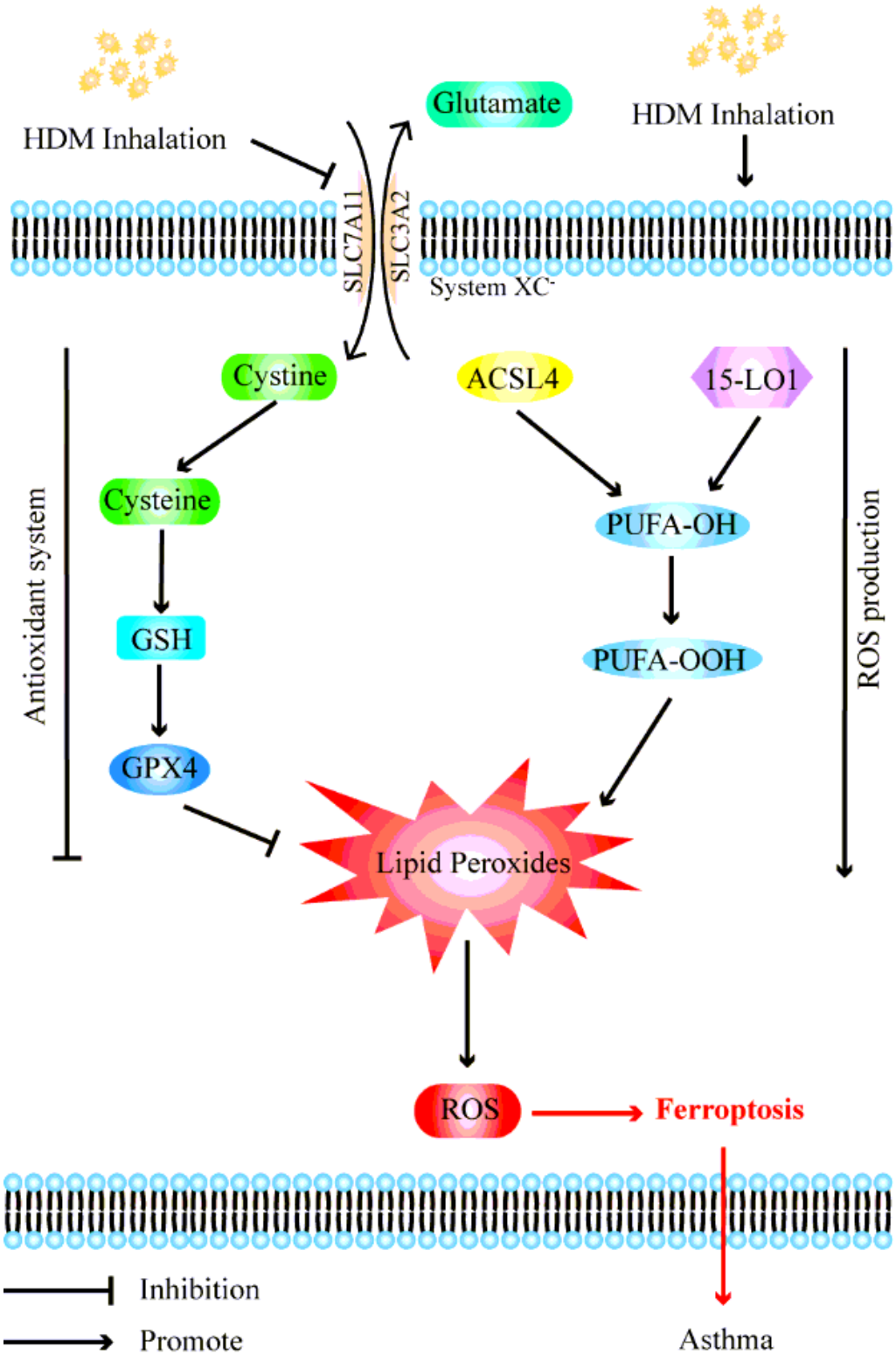

Figure 7

Pathways controlling ferroptosis in HDM-induced asthma pathogenesis